



Published in final edited form as:

*Toxicol In Vitro*. 2015 October ; 29(7): 1445–1453. doi:10.1016/j.tiv.2015.05.022.

## Systematic *in vitro* toxicological screening of gold nanoparticles designed for nanomedicine applications

Pratap C. Naha<sup>1</sup>, Peter Chhour<sup>1,2</sup>, and David P. Cormode<sup>1,2,3,\*</sup>

<sup>1</sup>Department of Radiology, University of Pennsylvania, 3400 Spruce St, 1 Silverstein, Philadelphia, PA 19104, USA

<sup>2</sup>Department of Bioengineering, University of Pennsylvania, 3400 Spruce St, 1 Silverstein, Philadelphia, PA 19104, USA

<sup>3</sup>Department of Cardiology, University of Pennsylvania, 3400 Spruce St, 1 Silverstein, Philadelphia, PA 19104, USA

### Abstract

Gold nanoparticles (AuNP) are increasingly being applied in the biomedical field as therapeutics, contrast agents, and in diagnostic systems, motivating investigations of their toxicity that might arise from accidental exposure. While other work has investigated the toxicological response to gold nanoparticles for industrial purposes, here we have surveyed formulations that have been developed for biomedical use, are in clinical trials or have been FDA-approved. The AuNP library tested contains a range of shapes, including spheres, rods and shells, that possess a range of coatings, such as silica, citrate, lipoprotein, polymaleic acid, polyethylene glycol, DNA and others. Good cytocompatibility for all formulations was observed after 1 hour of incubation. However after 24 hours exposure, a nanorod and a spherical DNA coated formulation resulted in toxicity. The coating material was the only factor that influenced toxicity. AuNP exposure seemed to have no effect on cell cytoskeleton deformation and cell spreading. Cell uptake, as measured by computed tomography and ICP-OES, as well as TEM images of cells, confirmed strong AuNP uptake for certain formulations, but there was no correlation with toxicity. No glove translocation occurred, therefore, nitrile gloves are an adequate safety precaution for working with the AuNP studied. In conclusion, the majority of AuNP formulations tested have very low adverse effects.

### Graphical Abstract

\*Corresponding Author: David P. Cormode, Ph.D, Tel: 215-615-4656, Fax: 240-368-8096, david.cormode@uphs.upenn.edu.

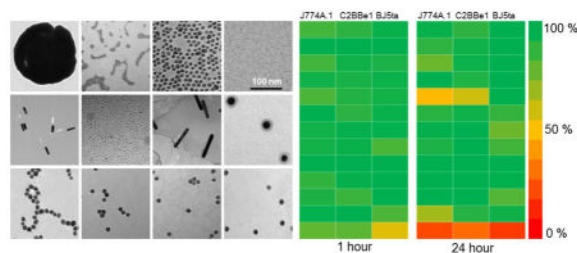
#### Conflict of interest

We have no conflict of interest to declare.

#### Supporting information

Synthesis of PMAL, m-PEG, HDL, 11-MUA, PEI and citrate coated AuNP, characterization of all the AuNP formulations, cell culture methodology, glove translocation assay, calculation of fractional deposition, higher magnification transmission electron micrographs of PMAL, Auro Vist and HDL AuNP, stability of AuNP in PBS, relationship between particle size, gold concentration and AuNP uptake with toxicity, transmission electron micrographs of C2BBE1 and J774A.1 cells incubated with PMAL, nanorod-1 and HDL coated AuNP and percent of administered dose internalized are available in the supporting information.

**Publisher's Disclaimer:** This is a PDF file of an unedited manuscript that has been accepted for publication. As a service to our customers we are providing this early version of the manuscript. The manuscript will undergo copyediting, typesetting, and review of the resulting proof before it is published in its final citable form. Please note that during the production process errors may be discovered which could affect the content, and all legal disclaimers that apply to the journal pertain.



## Keywords

nanotoxicology; gold nanoparticles; cytotoxicity; nanoparticle coating; nanomedicine

## Introduction

Gold nanoparticles (AuNP) are currently being widely explored in medicine as therapeutics,<sup>1–3</sup> drug/nucleic acid delivery platforms,<sup>4–6</sup> contrast agents<sup>7–12</sup> and in diagnostic systems.<sup>13,14</sup> AuNP have unique optical, electronic and surface properties<sup>15</sup> that have encouraged this trend. In addition, a favorable safety profile is expected due to the inert nature of elemental gold and to a history of gold compounds being used in medicine.<sup>16</sup> Some aspects of the effects of exposure have been investigated for AuNP, however, the formulations used in these studies are typically materials for industrial applications or would require several more coating and modification steps to make them biocompatible and suited for medicinal applications.<sup>17,18</sup> It has been shown that nanoparticle coating has a very significant effect on the biocompatibility of nanoparticles.<sup>19</sup> Therefore it is unlikely that the effects of accidental exposure to nanoparticles, whose purpose is industrial, will be the same for nanoparticles whose purpose is medicinal.

AuNP are now used in FDA-approved diagnostic devices,<sup>14</sup> clinical trials against cancer<sup>20</sup> and atherosclerosis<sup>21,22</sup> as well as a raft of pre-clinical medicinal applications.<sup>16</sup> AuNP are currently being developed and applied for a variety of medicinal applications.<sup>16,23</sup> A DNA labeled AuNP based system marketed by Verigene is now FDA-approved for a variety of diagnostic tests (technology based on that developed by the group of Mirkin).<sup>13,14</sup> Gold nanoshells are undergoing clinical trials in both head and neck cancer<sup>20</sup> and coronary artery disease<sup>21,22</sup> for the potential to ablate pathological tissue via a photothermal mechanism. A phase I clinical trial has been completed by Aurimmune using TNF $\alpha$  bound to AuNP in patients with advanced solid organ tumors.<sup>24</sup> The groups of Langer and Mirkin are pursuing gold nanoparticle nucleic acid delivery vectors.<sup>4,6</sup> Gold nanorods, due to their strong absorption and emission in the near-infrared window, have been proposed as both optical imaging agents and as photothermal-based therapeutics.<sup>3,7</sup> We<sup>9,25,26</sup> and others<sup>12,27,28</sup> are exploring AuNP as computed tomography (CT) contrast agents due to their strong X-ray attenuation properties. Rotello *et al* are developing a AuNP ‘nose’ based diagnostic system exploiting competitive binding to green fluorescent protein, allowing the detection of cancer protein signatures and bacteria.<sup>29,30</sup> The manufacture and use of AuNP for medicinal applications is therefore expanding. The possibility of exposure to the skin or ingestion from accidental spills or disposal of material during manufacturing is growing.

We have assembled a library of AuNP designed for biomedical applications via in house synthesis and acquisitions from commercial sources. Notably, the library contains oligonucleotide-coated nanoparticles approved by the FDA for genetic testing<sup>13</sup> and a gold nanoshell in clinical trials as an anti-cancer therapeutic.<sup>20</sup> The library contains a diverse array of formulations, covering the spectrum of applications, sizes, morphologies, and coatings, as summarized in Table 1. While small gold nanoparticles (<5 nm) will likely be easily excreted in the urine, and therefore may typically have an easier path to FDA approval, we included larger gold nanoparticles (>5 nm) in the study as some larger gold nanoparticles have been FDA-approved or are in clinical trials.<sup>20</sup> The AuNP were characterized in house using transmission electron microscopy (TEM), dynamic light scattering (DLS) and inductively coupled plasma optical emission spectroscopy (ICP-OES). The cytotoxicity of AuNP was determined against three mammalian cell lines, i.e., human fibroblasts (BJ5ta cell), human colon epithelial (C2BBE1 cell) and mouse macrophages (J774A.1 cells) using the MTS assay and cell cytoskeleton analysis. The internalization of AuNP in J774A.1, C2BBE1 and BJ5ta cells was investigated with computed tomography (CT), TEM and ICP-OES. The translocation of AuNP through nitrile gloves was investigated. Through these experiments we sought to determine the toxicity of the AuNP, sources of toxicity and possible protective measures.

## Materials and Methods

### Synthesis and characterization of AuNP

Synthesis of PMAL, m-PEG, HDL, 11-MUA, PEI and citrate coated AuNP and characterization of all the AuNP formulations are described in the supporting information.

### Cell viability

Cell culture methodology is described in the supporting information.

### Cytotoxicity assay

Cell viability of BJ5ta, C2BBE1 and J774A.1 cells was determined using the MTS ((3-(4,5-dimethylthiazol-2-yl)-5-(3-carboxymethoxyphenyl)-2-(4-sulfophenyl)-2H-tetrazolium) assay (CellTiter 96 cell proliferation assay kit; Promega, Madison, WI, USA). The assay was carried out in sterile 96 well flat bottom micro plates (Corning, NY, USA). In brief, 100  $\mu$ l of media at  $10^5$  cells/ml was seeded in each well of the 96 well plate and the plate was incubated at 37 °C in a 5% CO<sub>2</sub> humidified incubator for 24 hours. After 24 hours the cell monolayer was washed gently with sterile phosphate buffered saline (PBS) and then incubated with AuNP (2  $\mu$ l of AuNP per well from the stock) dispersed in the complete cell culture medium, whereas 100  $\mu$ l of 10% v/v dimethyl sulfoxide (DMSO) (Sigma-Aldrich) in complete cell culture medium was used as a positive control for all the cell lines. After 1 or 24 hours exposure, the media was removed and the cell monolayer was washed with sterile PBS. After washing, 20  $\mu$ l of MTS/phenazine methosulfate (PMS) solution and 100  $\mu$ l of cell culture medium was added to each well. After addition of MTS/PMS reagent, the 96 well plate was incubated at 37 °C in a 5% CO<sub>2</sub> humidified incubator for 1 hour and then the absorbance was measured at 490 nm using a micro plate reader. Three independent experiments were performed for each AuNP formulation in each cell line. The percentage of

cell viability was calculated as compared to untreated cells. Data are presented as mean  $\pm$  standard deviation (n=3). All the AuNP formulations were sterilized with 0.45  $\mu$ m syringe filter prior to performing cell viability experiments.

### Effect of AuNP on cell spreading and cell cytoskeleton

The effect of AuNP on the cell cytoskeleton and cell spreading was investigated in BJ5ta cells. This study was performed in a 35 mm glass bottom petri dish (In Vitro Scientific, Sunnyvale, CA, USA). In brief, 50,000 cells were seeded in a glass bottom petri dish and incubated at 37 °C in a 5% CO<sub>2</sub> humidified incubator for 24 hour. The cell monolayer was washed with sterile PBS and then incubated with different AuNP at the same concentration as above. After 1 hour of incubation the cells were washed twice with PBS and then fixed with 400  $\mu$ l of 4% paraformaldehyde (Electron Microscopy Sciences, Hatfield, PA, USA) for 20 minutes at room temperature. The cells were washed twice with PBS and then treated with 400  $\mu$ l of 0.1% Triton<sup>TM</sup> X-100 (Sigma-Aldrich) for 4 minutes. Next the cells were washed twice with PBS and blocked with 800  $\mu$ l of 1% BSA (Sigma-Aldrich) in PBS for 30 minutes. After blocking, the cells were incubated with primary antibody against  $\alpha$ -tubulin (1/150 dilution with blocking buffer, ab80779, abcam, Cambridge UK) for 2 hour at room temperature. The cells were washed thrice with blocking buffer and then incubated with secondary AF-488 conjugated goat anti-mouse antibody (1 drop in 500  $\mu$ l of blocking buffer, Life technologies, Grand Island, NY, USA) and AF-546 conjugated phalloidin (1/300 dilution, Life technologies) for 1 hour at room temperature. The cells were then washed thrice with PBS. 2 drops of prolong gold antifade reagent with DAPI (Life technologies) were added prior to imaging with a Nikon Eclipse fluorescence microscope (Nikon Eclipse Ti-U, Nikon Instruments Inc, Melville, NY, USA). A mercury bulb was used as the light source and UV, GFP (488 nm) and Ds-Red (556 nm) excitation filters were used for DAPI, tubulin and actin respectively. Fluorescence images were taken at 20x magnification and the images were merged using NIS-Elements microscope imaging software (Nikon Instruments Inc). The cell areas were calculated using Image J software for at least 50 cells per sample.

### Cellular uptake

The internalization of AuNP in BJ5ta, C2BBel and J774A.1 cells was examined using CT, ICP-OES and TEM. The cells were seeded in 6 well plates at a density of  $1.5 \times 10^6$  cells per well and allowed to adhere at 37 °C in a 5% CO<sub>2</sub> humidified incubator for 24 hours. The cells were then washed with PBS and incubated with 20  $\mu$ l of AuNP from stock dispersed in 1 ml of complete cell culture medium per well. After 24 hours, the media was removed and the cell monolayer was washed twice with PBS to remove non-internalized nanoparticles. BJ5ta, C2BBel cells were trypsinized, while cell scrapers were used to remove the J774A.1 cells. The cells were then centrifuged at 100 rcf for 5 minutes and the media was removed.

For CT imaging, cell pellets were re-dispersed in 100  $\mu$ l of 2% v/v glutaraldehyde and transferred to a 0.2 ml eppendorf tube. The cells were allowed to settle to form a loosely packed pellet. The resulting cell pellets were scanned using a Siemens Definition DS 64-slice clinical CT scanner and the CT images were analyzed using Osirix 64 bit (v3.7.1). The scanning parameters used were 100 kV (X-ray tube voltage) and 270 mA (X-ray tube current) with a matrix size of 512 $\times$ 512 cm and a slice thickness of 0.4 cm. The

reconstruction kernel used was U30u. For each AuNP and control three cell pellets were prepared. The CT attenuation in each set of cell pellets was recorded and averaged. Data are presented as mean  $\pm$  standard deviation (n=3).

For ICP-OES analysis of cells incubated with AuNP, cells were removed from the 6 well plates and then counted using a haemocytometer. The cells were then digested in 1 ml of aqua regia for 30 minutes in a 15 ml falcon tube. After 30 minutes treatment with acid, 9 ml of Milli-Q water was added to the tube to make the volume up to 10 ml. Then the tube was centrifuged at 1400 rcf for 5 minute to remove cell debris. The supernatant was collected and analyzed using the ICP-OES (Spectro Genesis ICP). For each AuNP and control three cell pellets were prepared. Data are presented as mean  $\pm$  standard deviation (n=3).

Transmission electron microscopy of cells incubated with selected AuNP formulations (i.e. PMAL, nanorod-1 and HDL coated AuNP) was performed using JEOL 1010 microscope. Cell pellets were prepared as above and then fixed with 2.5% glutaraldehyde. Cell sections were prepared using standard methods and were imaged using a JEOL 1010 microscope operating at 80 kV.

### **Glove translocation assay**

The glove translocation assay protocol is described in the supporting information.

## **Results**

### **Characterization of gold nanoparticles**

All the AuNP were characterized with DLS to measure their hydrodynamic diameters in deionized water and cell culture media. The PMAL, PEI and citrate coated AuNP seem to aggregate substantially in cell culture media. TEM was used to measure the gold core diameters, and ICP-OES was used for the determination of gold concentration in each AuNP formulation. This data is summarized in Table 1. TEM images of all AuNP formulations are shown in Figure 1. Higher magnification TEM images of PMAL, Auro Vist and HDL AuNP are shown in Figure S1. All the AuNP are found to remain suspended in phosphate buffer saline (PBS) pH 7.4 except citrate stabilized AuNP. After incubation of citrate stabilized AuNP in PBS, it precipitated and settled to the bottom of the vial (Figure S2). The core diameters of m-PEG, 11-MUA, PEI, citrate and DNA coated AuNP are 13–14 nm, whereas the core diameter of PMAL and HDL coated AuNP are around 5 nm. For the case of Auro Vist and gold nanoshells, the core diameter was found to be 3 and 145 nm respectively. DLS measurements typically gave diameters bigger than the diameters found from TEM measurements, as is usually observed. The hydrodynamic diameter of Auro Vist and nanorods could not be measured with DLS. Auro Vist is easily renally excretable, so its hydrodynamic size is presumably less than 5 nm.<sup>12</sup> Also, the anisotropy of nanorods means that their DLS measurements cannot be considered as their true physical dimensions.<sup>35</sup>

### **Effect of AuNP on cell viability**

Toxicological screening of the AuNP library was performed in J774A.1 (macrophage), C2BBel (epithelial) and BJ5ta (fibroblast) cells using the MTS assay. We used cell lines

that represent cells types that might be exposed to gold nanoparticles by ingestion, splashes or needle sticks. The MTS assay has been widely used for toxicological screening of many metal oxide and gold nanoparticles.<sup>36–40</sup> Among the 12 different types of AuNP screened for *in vitro* toxicity, none of the formations reduced cell viability more than 20% after a 1 hour exposure to AuNP (Figure 2). However, after 24 hours exposure, nanorod-1 decreased the cell viability of J774A.1 and C2BBE1 cells by as much as 50%. DNA coated AuNP also decreased the cell viability of macrophages by 30% after 24 hours exposure (Figure 2). Also the cytotoxicity was not dependent on either the AuNP size or the exposure concentrations, within the limits tested (Figure 3). We typically observed macrophages to be more sensitive to AuNP as compared to epithelial and fibroblast cells, likely due to their higher phagocytic activity and thus higher uptake of nanoparticles.

### Effect of AuNP on cell spreading and cell cytoskeleton

In addition to the cell viability study, we also examined the effect of each AuNP formulation on cell cytoskeleton deformation and cell spreading in BJ5ta cells after 1 hour exposure to AuNP. The cells were well spread even after treatment with AuNP and the cell morphology remained similar to the untreated (control) cells. The areas of 50 cells per sample were averaged, which showed that there was no substantial difference between control and AuNP treated cells (Figure 4). As a positive control we used cells treated with DMSO (20% v/v in complete cell culture media). This treatment had a significant adverse effect on actin and tubulin network, decreasing the cell area (Figure 4).

### Fractional deposition, cellular uptake and intracellular localization of AuNP

Analytical ultracentrifugation was performed to determine sedimentation coefficients in cell culture media. From this data we found the density of the gold nanoparticle aggregates in this medium, which allowed us to determine the fractional deposition of the nanoparticles as a function of time (Figure 5A). As can be seen, the deposition at 24 hours ranged from 44% for the PMAL/PEI coated AuNP to 88% for the HDL-AuNP. We plotted the fractional deposition at 24 hours with toxicity results (Figure 5B) but did not find a correlation between these variables.

AuNP uptake in J774A.1, BJ5ta and C2BBE1 cells was studied using CT, TEM and ICP-OES. AuNP produce strong X-ray attenuation, which is linear with concentration,<sup>41</sup> hence the cellular uptake of AuNP was first screened using a clinical CT scanner (Figure 6A and B). To confirm these results, and to probe uptake in a more sensitive fashion, we additionally analyzed the cell pellets with ICP-OES (Figure 6C). Greater nanoparticle uptake did not result in decreased cell viability (Figure 6D).

Intracellular localization of selected AuNP formulations was examined in the three cell lines in order to study whether differences in intracellular localization of AuNP caused differences in cell viability. We chose PMAL, nanorod-1 and HDL coated AuNP, as PMAL-coated AuNP are highly taken up, but have no effect on cell viability, whereas nanorod-1 has an adverse effect on cell viability, and HDL had no effect on cell viability and was not taken up very much under the conditions tested. After 24 hours incubation of PMAL, nanorod-1 and HDL coated AuNP, cells were prepared for examination with TEM.

Transmission electron micrographs of the BJ5ta cell sections are presented in Figure 7, which indicates that each type of nanoparticle accumulates in endosomes or lysosomes. We did not observe nanoparticles at the cell membrane. We also observed that the AuNP were localized in the endosomes or lysosomes of J774A.1 and C2BBel cells (Figure S3 and S4). These results are similar to previous reports.<sup>42</sup>

### Glove translocation assay

Nitrile gloves are commonly used in biomedical laboratories as personal protection from hazards. Although we found most of the formulations in the AuNP library to be biocompatible, we studied whether such gloves offer adequate protection against AuNP in a translocation assay. AuNP samples were placed for 1 hour on nitrile glove material that covered pieces of filter paper (Figure 8). Via both visual inspection and ICP-OES analysis, we found no AuNP in the filter papers. Furthermore, after washing, we found no gold adsorbed into the glove material itself either. These experiments suggest that nitrile gloves are an effective safety precaution during handling of AuNP that are designed for biomedical purposes.

### Discussion

The AuNP library includes AuNP of different surface coatings such as (PMAL (poly (maleic anhydride-alt-1-tetradecene), m-PEG (methoxy-polyethylene glycol), HDL (high density lipoprotein), 11-MUA (11-mercaptoundecanoic acid), citrate and others. The AuNP also have different sizes (3–145 nm) and morphologies (spheres, nanorods, and nanoshells). Citrate coated gold nanoparticles are not designed for biomedical applications, however we included them as a frequently used gold nanoparticle precursor.<sup>23</sup> Importantly, one formulation was extracted from cartridges used in an FDA-approved Verigene *in vitro* diagnostic system, while another is in clinical trials as a cancer therapeutic.<sup>20</sup> We subsequently studied the nanoparticles *in vitro* with samples taken at their stock concentrations. If a spill or accidental exposure occurs, it will happen at the stock concentration, therefore this is the most relevant concentration to test for toxicological assessment.

The cytotoxicity results suggest that the toxicity of the nanoparticles in our AuNP library is not dependent upon the particle size in three cell lines tested. We have evaluated the cytotoxicity of 3 nm (Auro Vist), 5 nm (PMAL and HDL coated AuNP), 15 nm (11-MUA, PEI, m-PEG, citrate, DNA coated AuNP), 41 nm (silica coated AuNP) and 145 nm (shells) AuNP and found that toxicity was not dependent on either the gold core diameter or the gold concentration, within the limits tested (Figure 3). When we performed linear regression fits to our data, the correlation coefficients were very low, i.e. less than 0.35, confirming no relation between toxicity and size/concentration (Figure S5). A recent study on gold nanoparticle toxicity by Soenen *et al.*, reported that, the toxicity of a 4 nm core poly (methacrylic acid) coated AuNP depends upon the exposure dose<sup>43</sup> and it is well-established that toxicity is typically dose dependent. However, the highest concentration formulations (Aurovist and m-PEG coated AuNP) are both designed for vascular phase CT imaging,

where very high doses are given. Hence they are designed to be tolerable at very high concentrations and we have not exposed the cells to a toxic dose of these agents.

Coating materials on the nanoparticle surface have a significant effect on biocompatibility.<sup>19</sup> In our study, we tested AuNP with different coating materials such as PMAL, m-PEG, PEI, 11-MUA, HDL, DNA and Silica. To coat AuNP with ligands, the molecule is selected such that part of it binds strongly to the gold surface, whereas the other part is exposed to yield the desired solubility and interactions with the surroundings. For example, for m-PEG thiol capped AuNP, PEG functionalities are included to be on the nanoparticle exterior to increase its circulation half-life, while the thiol functionality is adsorbed on the gold surface and does not interact with the environment. Toxicity screening of nanoparticles conjugated with capping agents is therefore likely the best methodology to determine the role of capping agent on nanoparticle toxicity/biocompatibility. Even though the exposure dose of DNA coated AuNP is at least 50 times lower than the other AuNP, these reduced the J774A.1 cell viability around 30% after 24 hours of incubation. From our data, the nanoparticle coating seems to be the major factor in determining toxicity. However, we only surveyed a limited sample of AuNP, so other factors such as size or shape may play a greater role under some circumstances. Interestingly, we found that gold nanorod-1 (9 × 28 nm) adversely affected the cell viability of J774A.1 and C2BBel while larger gold nanorods (nanorod-2, 13 × 84 nm) had no adverse effect on cell viability. Potentially, the larger surface area of the smaller nanorods could be the cause of the stronger toxicity of the smaller nanorods. The DNA coated AuNP used in the Verigene diagnostic system reduced cell viability after 24 hours. However, it is worth noting that these nanoparticles are not designed for *in vivo* use, but for an *in vitro* diagnostic assay. In addition, there may be other chemicals in the solution to facilitate this assay. Such chemicals might be the cause of the effect on cell viability, as opposed to the gold nanoparticles. Since the main effect on toxicity we observed seemed to arise from the coating, it will be important to probe the effect of coating with other nanoparticle core types such as iron oxide, silica and so forth.

It has previously been reported that certain AuNP formulations can cause the deformation of cell cytoskeleton networks after incubation with different cell types.<sup>43–46</sup> Although most of the AuNP formulations in the AuNP library were found to be biocompatible, we explored whether the formulations induced a more subtle adverse effect on the cells, such as cytoskeleton deformation.<sup>45</sup> Our results suggest that exposure to the AuNP in our library had no adverse effect on tubulin or actin filaments (Figure 4).

Among all the AuNP studied, cells incubated with 11-MUA and PMAL coated AuNP produced strong (>100 HU increase) CT attenuation, which indicates high levels of uptake of nanoparticles (Figure 6B). ICP-OES results broadly agree with those from the CT data, *i.e.* that larger amounts of 11-MUA and PMAL nanoparticles were internalized than other formulations (Figure 6C). The AuNP library contains varieties of formulations that differ in size, surface coatings and morphology. While there is variation in the stock concentrations of the nanoparticles used, which will affect the levels of cell uptake, we can draw some conclusions from trends in our data. The coating materials of the AuNP seemed to have the most significant role in cell uptake. For example, high levels of cell uptake were found with 11-MUA AuNP, while PEI coated AuNP of the same concentration and PEG coated AuNP



of about eightfold higher concentration, were taken up much less. Each of the above formulations had the same core size. Similarly, PMAL coated AuNP were avidly taken up by the cells, whereas HDL and Auro Vist, which had similar core sizes were taken up less. Interestingly, when compared to the toxicity data (Figure 2), we found no correlation between cell uptake and effect on viability (Figure S6, correlation coefficients from linear fits are less than 0.15). The percentage of AuNP internalized in cells compared to exposure dose was calculated and we found that higher percentages of 11-MUA and PMAL coated AuNP were internalized than other AuNP tested (Figure S7). Formulations that were strongly taken up by the cells (11-MUA, PMAL) had no effect on cell viability, whereas some formulations that were taken up to only a slight extent (DNA coated, Nanorod-1) produced marked decreases in cell viability.

Some of the AuNP tested here have been previously studied for their biocompatibility. It has been reported that 1.9 nm AuNP<sup>47</sup> and 15 nm AuNP coated with m-PEG did not produce any adverse effect in mice.<sup>32</sup> In vitro toxicity of 15 nm AuNP coated with 11-MUA,<sup>33</sup> HDL coated AuNP,<sup>5</sup> PEI capped 15 nm AuNP,<sup>34</sup> silica coated AuNP<sup>16</sup> and a 153 nm PEGylated gold nanoshells<sup>48</sup> are found to be cytocompatible in a range of cell lines and under a range of conditions. Another in vitro study reported that cetyltrimethylammonium bromide coated gold nanorods reduce the HeLa cell viability 21%, whereas for the case of polyelectrolytes (such as poly(diallyldimethylammonium chloride)–poly(4-styrenesulfonic acid) coated gold nanorods are cytocompatible.<sup>49</sup> However, the range of models, cell lines and conditions used in these previous reports underscores the importance of systematic studies such as ours for the exploration of toxicity.

Our results show that, most of the AuNP tested have very low adverse effects therefore, excessive precautions are likely not needed in sites of synthesis, in transport and in locations of use. When designing our experiments, we primarily had exposures via splashes onto skin or accidental ingestion in mind. We would argue that our experiments also give some guidance to exposures via needle sticks. Our experiments do not model exposures to the eye, which could occur during transportation of nanoparticles or if they are used in clinical situations (laboratories typically mandate the use of safety glasses, therefore in these settings the risk is less). Future work should include experiments that model exposure of nanoparticles to the eye. In this study we used macrophage, fibroblast and epithelial cells. Future work might explore the use of alternative cell lines or cell types. It is worth pointing out that we surveyed a relatively small portion of the AuNP that have been reported for biomedical applications.<sup>23</sup> Each agent that moves towards the clinic will need to be studied on an individual basis for its toxicology. Nevertheless, our sample covered a wide range of nanoparticle sizes, shapes and coatings and our data suggests that there is not a strong reason for concern. Others have observed toxic reactions from gold nanoparticles under certain conditions,<sup>17,42,50,51,52</sup> however, such formulations are not typically specifically designed for biomedical formulations. Moreover, although any material will prove toxic at some concentration, the relevant test for toxicity is at the concentration of the material when in transport or at the point of use, as tested here. If we had studied higher concentrations of agents, we would likely have eventually found concentrations at which toxicity occurs.

## Conclusions

In summary, our results suggest that most of the AuNP tested are highly cytocompatible, except a nanorod and a DNA coated nanosphere. ICP-OES, CT and TEM indicate that some AuNP are avidly internalized in the cells and localize to lysosomes/endosomes. The amount of AuNP uptake in cells was primarily a function of the surface coating material rather than particle size, for the materials surveyed. Importantly, the extent of uptake does not seem to correlate to toxicity. The toxicity of the AuNP also seems to primarily depend upon the coating materials rather than particle size, and exposure dose. We observed that AuNP cannot penetrate through nitrile gloves, therefore the standard safety measure of using nitrile gloves is effective for use during handling of AuNP designed for biomedical purposes. Further AuNP toxicological assessments need to be done, and each new nanoparticle formulation needs to be studied on a case-by-case basis.

## Supplementary Material

Refer to Web version on PubMed Central for supplementary material.

## Acknowledgments

This work was supported by the Penn Nanotoxicology Alliance (Nanotechnology Institute, Nano-Biointerface Center, Center for Translational Targeted Therapeutics and Nanomedicine, and the Center of Excellence in Environmental Toxicology –P30ES13508) with funds from the Provost. The project described was supported in part by the Institute for Translational Medicine and Therapeutics (ITMAT) Transdisciplinary Program in Translational Medicine and Therapeutics (Grant Number UL1RR024134 from the National Center for Research Resources. The content is solely the responsibility of the authors and does not necessarily represent the official views of the National Center for Research Resources or the National Institutes of Health). We acknowledge additional funding from NIH Grant R00 EB012165 and startup funds from the University of Pennsylvania. We thank Trevor Penning for his insightful suggestions with regards the experimental design and Harold Litt for assistance with CT image acquisition (both of the University of Pennsylvania). We thank Sriram Krishnaswamy of the University of Pennsylvania for his help in measuring sedimentation coefficients.

## References

1. Huang X, et al. *J Am Chem Soc.* 2006; 128:2115. [PubMed: 16464114]
2. Kim J, et al. *Angew Chem Int Ed Engl.* 2006; 45:7754. [PubMed: 17072921]
3. O'Neal DP, et al. *Cancer Lett.* 2004; 209:171. [PubMed: 15159019]
4. Lee JS, et al. *Nano Lett.* 2009; 9:2402. [PubMed: 19422265]
5. McMahon KM, et al. *Nano Lett.* 2011; 11:1208. [PubMed: 21319839]
6. Rosi NL, et al. *Science.* 2006; 312:1027. [PubMed: 16709779]
7. Durr NJ, et al. *Nano Lett.* 2007; 7:941. [PubMed: 17335272]
8. Qian X, et al. *Nat Biotechnol.* 2008; 26:83. [PubMed: 18157119]
9. Cormode DP, et al. *Radiology.* 2010; 256:774. [PubMed: 20668118]
10. Alric C, et al. *J Am Chem Soc.* 2008; 130:5908. [PubMed: 18407638]
11. Cormode DP, et al. *Nano Lett.* 2008; 8:3715. [PubMed: 18939808]
12. Hainfeld JF, et al. *Br J Radiol.* 2006; 79:248. [PubMed: 16498039]
13. Rosi NL, Mirkin CA. *Chem Rev.* 2005; 105:1547. [PubMed: 15826019]
14. Hallouard F, et al. *Biomaterials.* 2010; 31:6249. [PubMed: 20510444]
15. Daniel MC, Astruc D. *Chem Rev.* 2004; 104:293. [PubMed: 14719978]
16. Thakor AS, et al. *Nano Lett.* 2011; 11:4029. [PubMed: 21846107]
17. Alkilany AM, et al. *Small.* 2009; 5:701. [PubMed: 19226599]

18. Yen HJ, Hsu SH, Tsai CL. *Small*. 2009; 5:1553. [PubMed: 19326357]
19. van Schooneveld MM, et al. *Nano Lett*. 2008; 8:2517. [PubMed: 18624389]
20. Pilot Study of AuroLase(T<sup>M</sup>) Therapy in Refractory and/or Recurrent Tumors of the Head and Neck. <http://clinicaltrials.gov/ct2/show/NCT00848042>, (Clinical trial identifier: NCT00848042)
21. Plasmonic Nanophotothermic Therapy of Atherosclerosis (NANOM). <http://clinicaltrials.gov/ct2/show/NCT01270139>, (Clinical trial identifier: NCT01270139)
22. Plasmonic Photothermal and Stem Cell Therapy of Atherosclerosis Versus Biodegradable Stenting (NANOM2). <http://clinicaltrials.gov/ct2/show/NCT01436123>, (Clinical trial identifier: NCT01436123)
23. Mieszawska AJ, et al. *Mol Pharm*. 2013; 10:831. [PubMed: 23360440]
24. Libutti SK, et al. *Clin Cancer Res*. 2010; 16:6139. [PubMed: 20876255]
25. van Schooneveld MM, et al. *Contrast Media Mol Imaging*. 2010; 5:231. [PubMed: 20812290]
26. Allijn IE, et al. *ACS Nano*. 2013; 7:9761. [PubMed: 24127782]
27. Chanda N, et al. *Proc Natl Acad Sci U S A*. 2010; 107:8760. [PubMed: 20410458]
28. Jackson PA, et al. *Eur J Radiol*. 2010; 75:104. [PubMed: 19406594]
29. Bajaj A, et al. *Proc Natl Acad Sci U S A*. 2009; 106:10912. [PubMed: 19549846]
30. You CC, et al. *Nat Nanotechnol*. 2007; 2:318. [PubMed: 18654291]
31. Cormode DP, et al. *Bioconj Chem*. 2011; 22:353.
32. Cai QY, et al. *Invest Radiol*. 2007; 42:797. [PubMed: 18007151]
33. Chien CC, et al. *Scientific Reports*. 2012; 2:610. [PubMed: 22934133]
34. Song WJ, et al. *Small*. 2010; 6:239. [PubMed: 19924738]
35. Liu H, Pierre-Pierre N, Huo Q. *Gold Bulletin*. 2012; 45:187.
36. Chuang SM, et al. *Biochim Biophys Acta*. 2013; 1830:4960. [PubMed: 23811345]
37. Freese C, et al. *Part Fibre Toxicol*. 2012; 9:23. [PubMed: 22759355]
38. Schaeublin NM, et al. *Langmuir*. 2012; 28:3248. [PubMed: 22242624]
39. Schaeublin NM, et al. *Nanoscale*. 2011; 3:410. [PubMed: 21229159]
40. Zhang H, et al. *ACS Nano*. 2012; 6:4349. [PubMed: 22502734]
41. Galper MW, et al. *Invest Radiol*. 2012; 47:475. [PubMed: 22766909]
42. Chithrani BD, Ghazani AA, Chan WCW. *Nano Lett*. 2006; 6:662. [PubMed: 16608261]
43. Soenen SJ, et al. *ACS Nano*. 2012; 6:5767. [PubMed: 22659047]
44. Coradeghini R, et al. *Toxicol Lett*. 2013; 217:205. [PubMed: 23246733]
45. Huang X, et al. *Biomaterials*. 2010; 31:438. [PubMed: 19800115]
46. Wu YL, et al. *Acc Chem Res*. 2013; 46:782. [PubMed: 23194178]
47. Simpson CA, et al. *Nanomedicine*. 2013; 9:257. [PubMed: 22772047]
48. Liu H, et al. *Biomaterials*. 2013; 34:6967. [PubMed: 23777913]
49. Hauck TS, et al. *Small*. 2008; 4:153. [PubMed: 18081130]
50. Bar-Ilan O, et al. *Small*. 2009; 5:1897. [PubMed: 19437466]
51. Alkilany AM, Lohse SE, Murphy CJ. *Acc Chem Res*. 2013; 46:650. [PubMed: 22732239]
52. Pan Y, et al. *Small*. 2007; 3:1941. [PubMed: 17963284]

### Highlights

1. A library of AuNP designed for biomedical applications was studied.
2. The physical characteristics of this library were thoroughly evaluated.
3. The biocompatibility, uptake and localization were tested in three cell lines.
4. The toxicity of the AuNP tested depended on the coating materials.
5. These AuNP cannot penetrate though nitrile gloves.

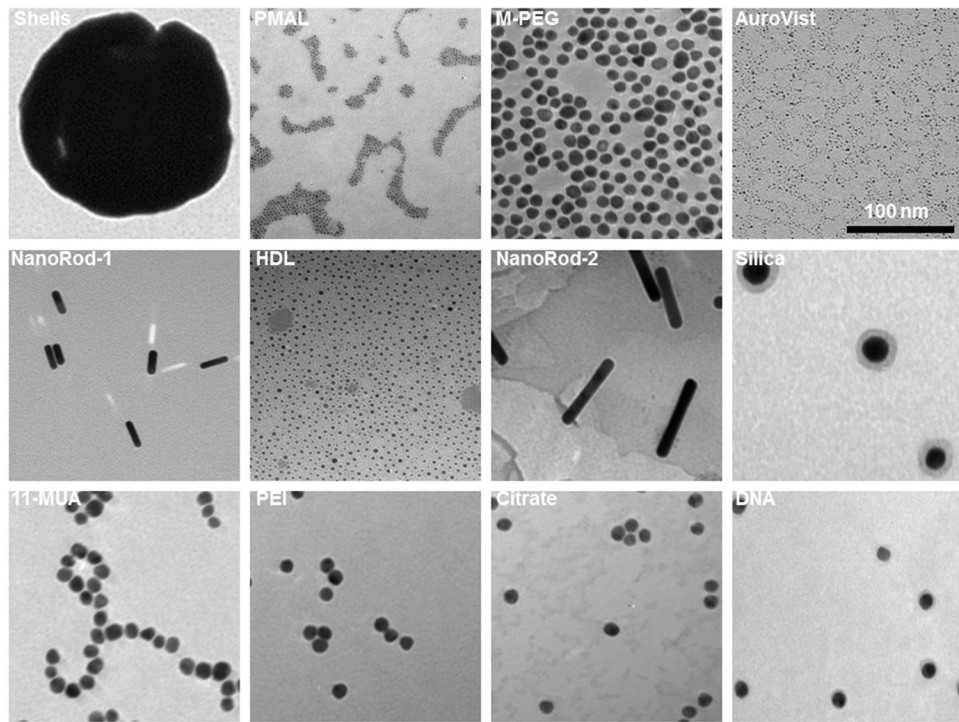


**Figure 1.** Transmission electron micrographs of AuNP library. The scale is the same in all panels.

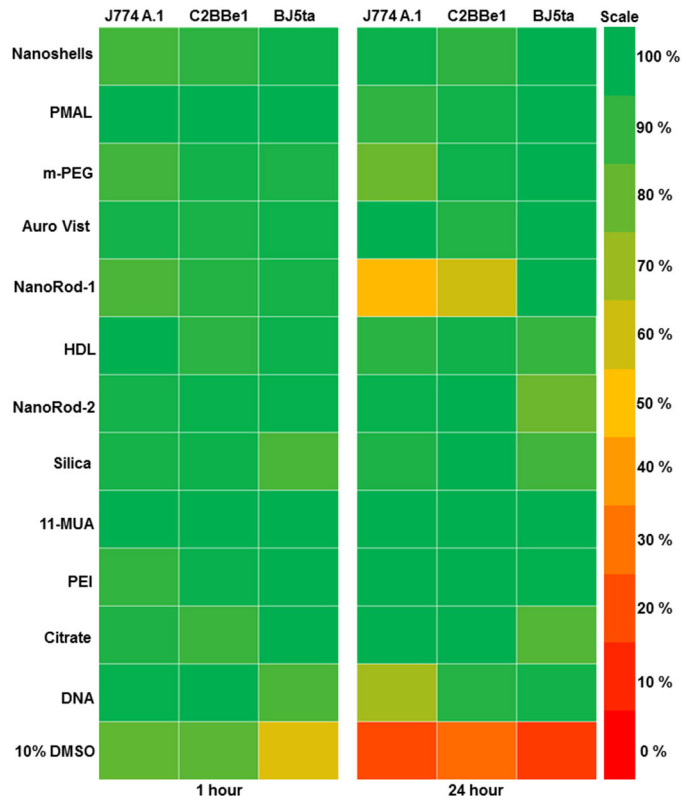


**Figure 2.** Heat map showing relative cell viability of J774A.1, C2BBE1 and BJ5ta cells after exposure to AuNP library for 1 and 24 hours. Red represents 0% cell viability (all the cells are dead) and green represents 100% cell viability (all the cells are live). Percentage of viability was determined compared to control.

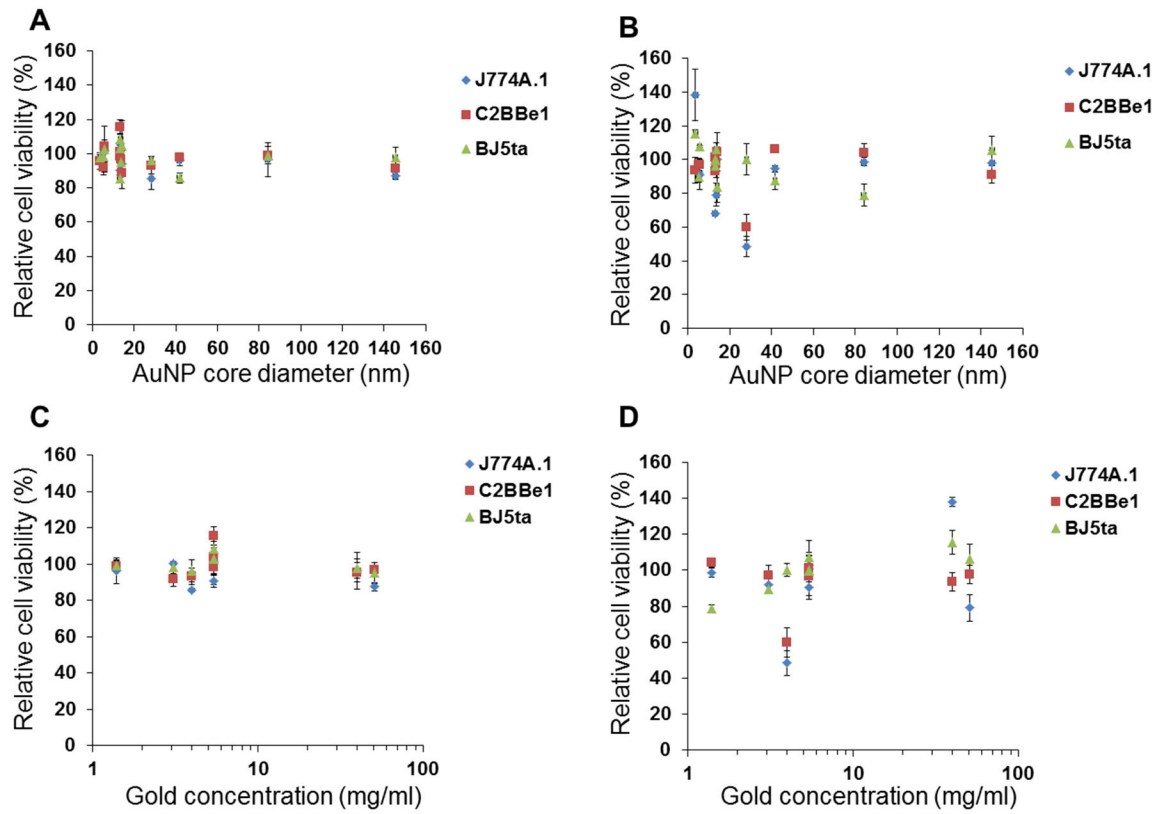


**Figure 3.** Plots of cell viability versus AuNP size for A) 1 and B) 24 hours of incubation. Plots of cell viability versus AuNP concentration for C) 1 and D) 24 hours of incubation. Error bars are one standard deviation.

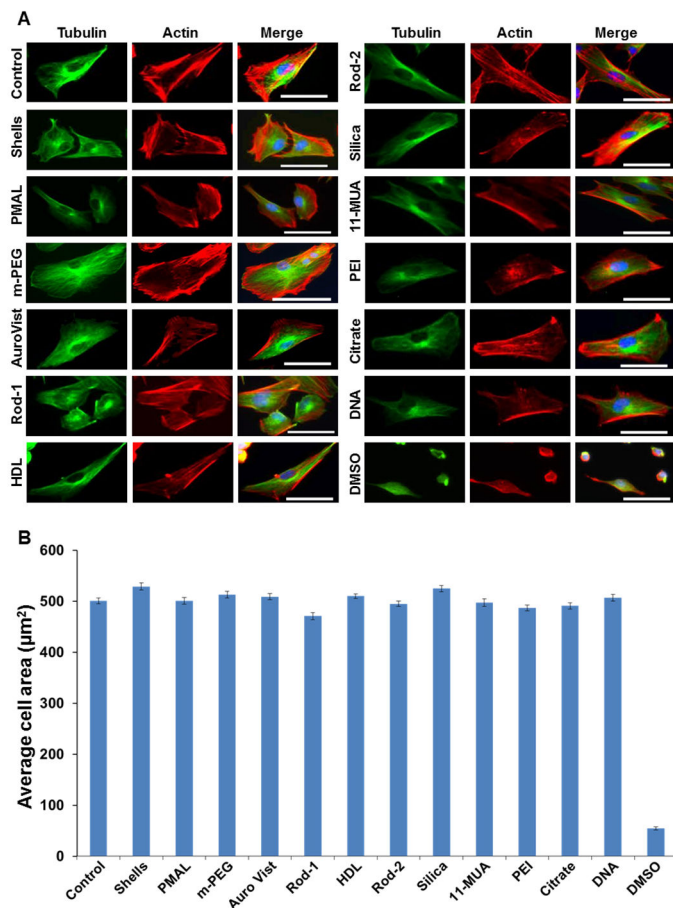


**Figure 4.** Effect of AuNP on cell cytoskeleton and cell spreading. A) Representative fluorescence micrographs of BJ5ta cells stained for actin (red) and tubulin (green). The nuclei are stained with DAPI (blue). Scale bar is 25 µm. Panel B, graph showing the average cell area after 1 hour exposure of AuNP to the BJ5ta cells. The cell area was calculated using Image J software. Error bars are the standard error of mean.



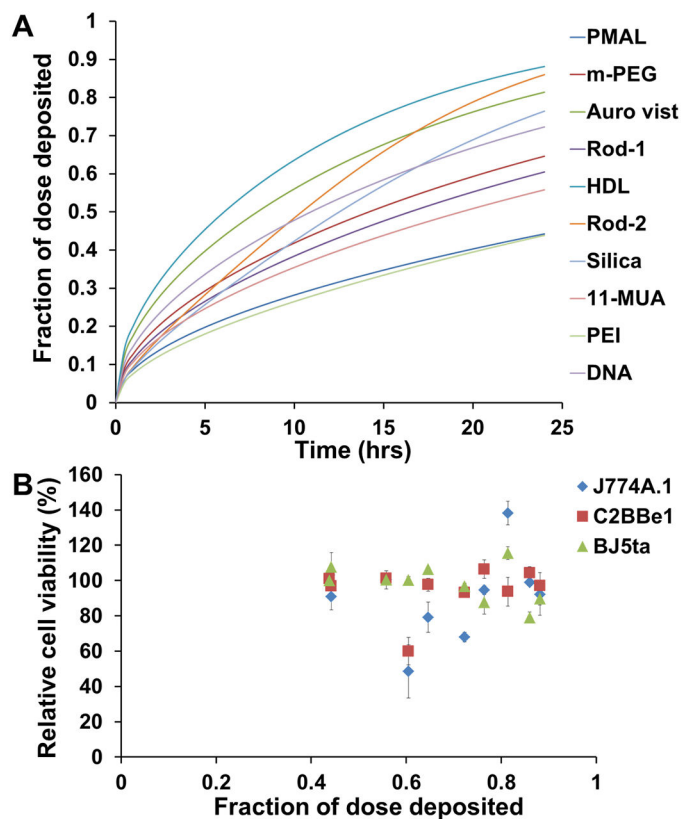


**Figure 5.** A) Fractional deposition of AuNP as a function of time. B) Relationship between cytotoxicity and fraction of dose deposited at 24 hours (B). Error bars are one standard deviation.

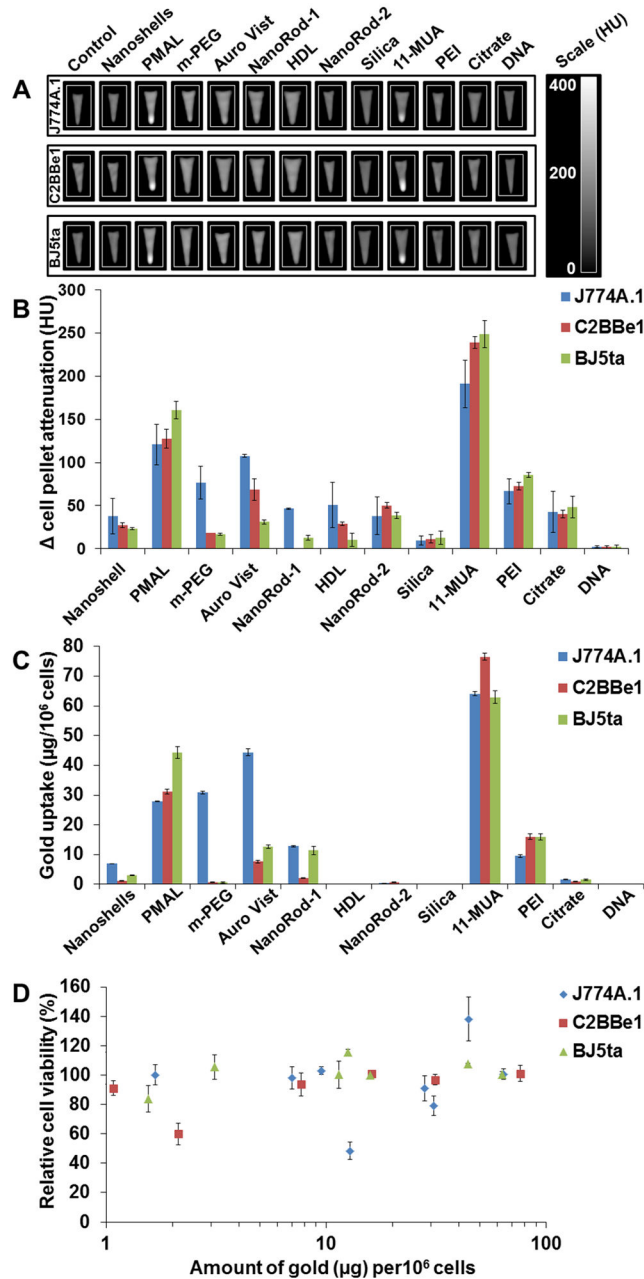


**Figure 6.**

A) CT images of pellets of cells incubated with AuNP formulations. B) Quantification of CT attenuation from images in A). C) AuNP uptake after 24 hours incubation with J774A.1, C2BBe1 and BJ5ta cells measured using ICP-OES. D) Relationship between toxicity and AuNP uptake. Error bars are one standard deviation.

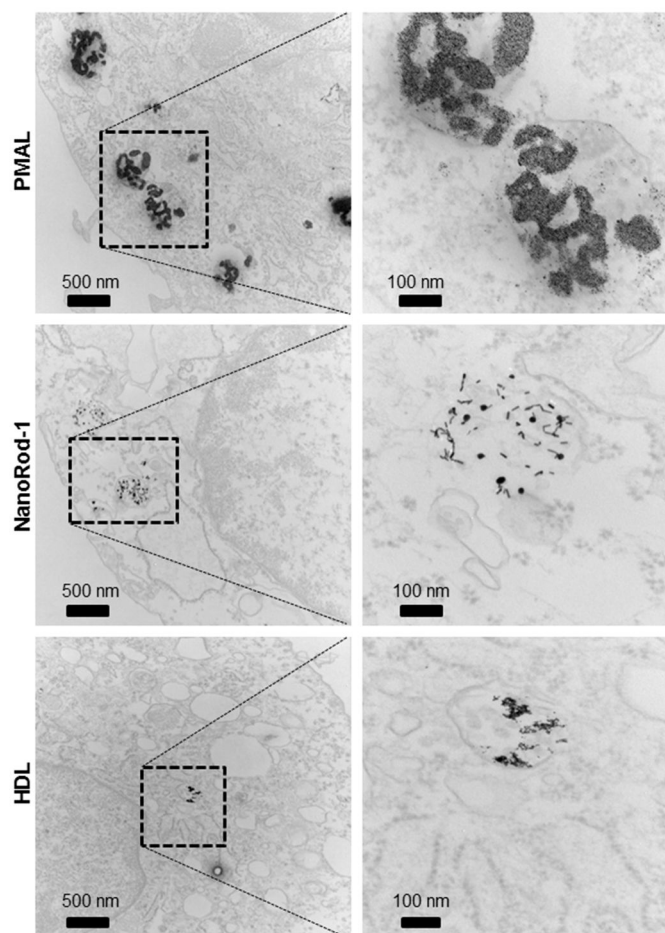


**Figure 7.** Transmission electron micrographs of BJ5ta cells incubated with PMAL, Nanorod-1 and HDL coated AuNP.

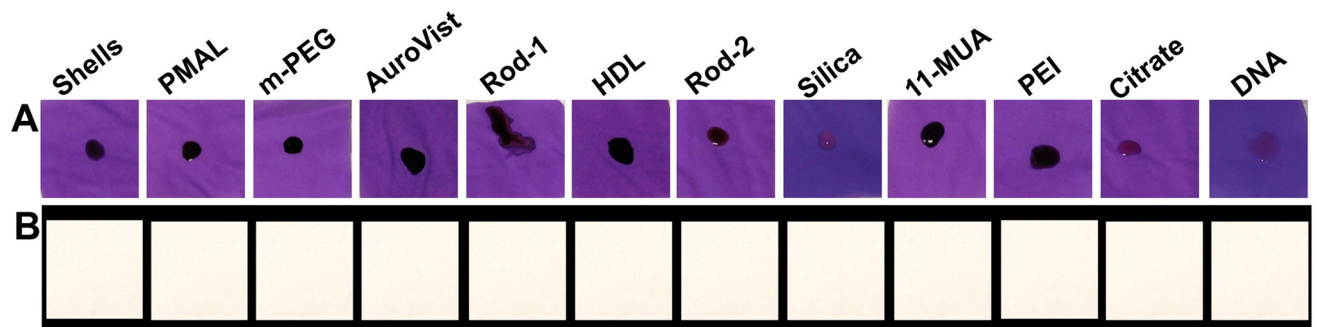


**Figure 8.**

Investigation of the ability of AuNP to penetrate through nitrile gloves. A) photographs of pieces of nitrile gloves spotted with 10  $\mu$ l of AuNP, which were placed over pieces of filter paper. B) photographs of pieces of filter paper after 1 hour of incubation with AuNP on nitrile glove material above them.

**Table 1**

Description of the AuNP library, such as coating materials, morphology, characterization results and applications of each formulation.

AuNP Formulations	Morphology	Gold content in mg/ml	Hydrodynamic diameter in MQ water (nm)	Hydrodynamic diameter in cell culture media (nm)	Core diameter (nm)	Zeta potential (mV)	Applications and source	References
Gold nanoshells	Shell	0.9	169 ± 0.5	157 ± 1.5	145.4 ± 12.1	-41 ± 0.8	Therapeutics/fluorescence (Nanocompositox)	3
Polymer († PMAL)	Spherical	5.4	85 ± 31	303 ± 2.7	5.7 ± 1.5	+44 ± 3	CT cell labelling (in house)	31
† m-PEG	Spherical	51	20.6 ± 0.11	17.49 ± 0.12	13.7 ± 2	-29 ± 0.5	Vascular CT (in house)	32
Auro Vist™	Spherical	40.1	*	19 ± 0.9	3.6 ± 1.2	-13 ± 1.5	Vascular CT (Nanoprobes)	12
† Methyl	Rod-1	4	*	-	28.1 ± 1.3 (Length) 9.1 ± 4 (Width)	-13 ± 1.4	Therapeutics/fluorescence (Nanopartz)	7
† HDL	Spherical	3.1	13.2 ± 2.8	12 ± 2	5.1 ± 1	-9 ± 1.3	Targeted CT (in house)	9
† Methyl	Rod-2	1.4	*	-	84 ± 16.9 (Length) 13.6 ± 2.5 (Width)	-21 ± 3.7	Therapeutics/fluorescence (Nanopartz)	7
† Silica	Spherical	0.03	77.3 ± 1.1	49 ± 1.7	41.7 ± 3.4	-44 ± 0.6	Therapeutics (Nanopartz)	25
† 11-MUA	Spherical	5.4	60.6 ± 6.3	60 ± 0.5	13.3 ± 1.5	-45 ± 0.9	CT cell labelling (in house)	33
† PEI	Spherical	5.4	26 ± 7.2	145 ± 15	13.2 ± 2.0	+47 ± 1	Therapeutics (in house)	34
† Citrate	Spherical	0.3	14 ± 1	31 ± 0.3	13.5 ± 1.8	-29 ± 1.5	Raw material (in house)	32
† DNA	Spherical	0.01	28.3 ± 0.5	15.4 ± 0.9	13 ± 1.9	-3.5 ± 1.5	Diagnostics (Nanosphere)	13

† denotes coating materials.

\* denotes that hydrodynamic diameter measurements of these formulations were not possible with DLS, see results section for explanation.